Circular Rydberg States of the Hydrogen Atom in a Magnetic Field

Timothy C. Germann and Dudley R. Herschbach
Department of Chemistry, Harvard University, Cambridge, Massachusetts 02138

Martin Dunn and Deborah K. Watson
Department of Physics and Astronomy, University of Oklahoma, Norman, Oklahoma 73019
(Received 9 September 1994)

Dimensional perturbation theory is used to study circular Rydberg states ($|m| = n - 1 \gg 1$) and other large $|m|$ states of the hydrogen atom in a uniform magnetic field. Because of a degeneracy between states of increased angular momentum and states of increased Cartesian dimensionality, the accuracy of the zeroth-order $D \to \infty$ limit and a dimensional perturbation expansion improves significantly for states with larger $|m|$. In contrast to other approaches, this method is applicable to the entire range of magnetic field strengths. Energies and expectation values are presented as functions of the field strength.

PACS numbers: 32.60.+i, 31.50.+w

Dimensional scaling methods that employ the dimensionality D of space as a variable have proved effective in treating nonseparable problems which lack a natural expansion parameter [1]. The $D \to \infty$ limit often permits an exact solution that can be used to derive accurate $D = 3$ results from a perturbation expansion in powers of $1/D$ [2]. Kindred perturbation expansions have been applied to atoms in external fields, primarily by Popov and coworkers [3]. The hydrogen atom in a uniform magnetic field has been treated by Bender *et al.* [4], who derived a semiclassical expansion for the ground state energy in powers of $(2|m| + 2)^{-1}$, where m is the azimuthal quantum number. Recently, dimensional perturbation theory (DPT) has been applied to this problem, exploiting a new algorithm [5] that facilitates high order calculations [6]. Here we report calculations for circular Rydberg states ($|m| = n - 1 \gg 1$) and other large $|m|$ states.

Since the D and $|m|$ dependences enter the Schrödinger equation only in the factor $\kappa \equiv D + 2|m| - 1$, i.e., enter the physics in equivalent and interchangeable ways, interdimensional degeneracies are found between states with angular momentum $|m|$ in D dimensions and states with angular momentum $|m| - x$ in $D + 2x$ dimensions. An expansion in powers of $1/\kappa$ provides a perturbation theory which is explicitly invariant under these interdimensional degeneracies, i.e., *DPT is equivalent to angular momentum perturbation theory about* $|m| \to \infty$. At $D = 3$, this is identical to the expansion of Bender *et al.* [4]. Multielectron systems also display interdimensional degeneracies, however, the complete equivalence of angular momentum and dimensionality is no longer present.

Unlike other methods, such as variational methods employing spherical or Landau basis functions, DPT is an effective method for all magnetic field strengths. This is because every term in the Hamiltonian is involved, at least approximately, in the equation for the zeroth-order wave function. The accuracy of such a perturbation expansion has been demonstrated for the lowest (nodeless) state in the $|m| = 0$ and 1 manifolds [4,6]. However, the method becomes even more powerful for states with large $|m|$ and hence small $1/\kappa$, because the zeroth-order approximation is the classical ($|m| \to \infty$) orbit along a circle perpendicular to the magnetic field (z) axis.

Circular Rydberg states (CRS) have received much attention. Such states were first obtained by Hulet and Kleppner [7] and new preparative methods continue to be devised [8]. Among the unique features of CRS are long radiative lifetimes and highly anisotropic collision cross sections. Since the only available dipole transitions connect neighboring CRS, these states enable studies of atom-cavity effects such as inhibited spontaneous emission [9]. The semiclassical nature of circular eigenstates [3] has been investigated in studies of circular-orbit wave packet dynamics [10]. Calculations for CRS have been made by Wunner *et al.* [11], by expanding the wave function in terms of spherical harmonics, the natural basis for the weak-field limit. From large scale computations, they evaluated energies, transition frequencies, and radiative decay times for $|m| = 24$ to 35 and $B \leq 70.5$ T, while energies for superstrong fields ($\leq 10^7$ T) were obtained using the adiabatic approximation [12]. In contrast to that work, DPT requires modest calculations and is applicable to the entire range of magnetic field strengths.

The Schrödinger equation for a D-dimensional nonrelativistic hydrogenic atom in a uniform magnetic field along the z axis, in a.u. and cylindrical coordinates, is

$$\left\{-\frac{1}{2}\delta^2\left(\frac{\partial^2}{\partial\tilde{\rho}^2}+\frac{\partial^2}{\partial\tilde{z}^2}\right)+\frac{1-4\delta+3\delta^2}{8\tilde{\rho}^2}+\frac{\tilde{B}^2\tilde{\rho}^2}{8}-\frac{Z}{\sqrt{\tilde{\rho}^2+\tilde{z}^2}}\right\}\Phi(\tilde{\rho},\tilde{z})=\epsilon\Phi(\tilde{\rho},\tilde{z}), \quad (1)$$

where $\rho = \kappa^2\tilde{\rho}$, $z = \kappa^2\tilde{z}$, $\tilde{B} = \kappa^3 B$, $\epsilon = \kappa^2 E$, and $\delta = 1/\kappa$ is treated as a continuous perturbation parameter [6]. The magnetic field strength B is measured in units $m_e^2 e^3 c/\hbar^3 \simeq 2.35 \times 10^9$ G, and the Zeeman term $mB/2$ is omitted since it does not affect the dynamics.

 0031-9007/95/74(5)/658(4)$06.00

In the limit $\delta \to 0$ the Schrödinger equation reduces to a potential problem with an effective potential

$$V_{\rm eff}(\tilde{\rho},\tilde{z}) = \frac{1}{8\tilde{\rho}^2} + \frac{\tilde{B}^2\tilde{\rho}^2}{8} - \frac{Z}{\sqrt{\tilde{\rho}^2+\tilde{z}^2}}. \quad (2)$$

Thus DPT identifies the leading approximation with the minimum of $V_{\rm eff}(\tilde{\rho},\tilde{z})$ at $\tilde{\rho} = \rho_m$ and $\tilde{z} = z_m = 0$ and fluctuations about this minimum with higher order corrections in powers of δ. Displacements from this rigid structure may be incorporated by introducing dimension-scaled displacement coordinates $x_1 = (\tilde{\rho} - \rho_m)/\delta^{1/2}$ and $x_2 = \tilde{z}/\delta^{1/2}$. This leads to [6]

$$\left[V_{\rm eff}(\rho_m,0) + \delta \sum_{j=0}^{\infty} \delta^{j/2} \mathcal{H}_j - \epsilon \right] \Phi(x_1,x_2) = 0, \quad (3)$$

where

$$\mathcal{H}_0 = -\frac{1}{2}\left(\frac{\partial^2}{\partial x_1^2} + \frac{\partial^2}{\partial x_2^2}\right) + \frac{1}{2}\omega_1^2 x_1^2 + \frac{1}{2}\omega_2^2 x_2^2 - \frac{1}{2\rho_m^2},$$

$$\omega_1^2 = \frac{3}{4\rho_m^4} - \frac{2Z}{\rho_m^3} + \frac{\tilde{B}^2}{4}, \qquad \omega_2^2 = \frac{Z}{\rho_m^3},$$

$$\mathcal{H}_{j>0} = \left(\sum_{l=0}^{(j+2)/2} {}^{l}v_{j,j+2} x_1^{j+2-2l} x_2^{2l} \right) + v_{j,j} x_1^j + v_{j,j-2} x_1^{j-2}.$$

$\mathcal{H}_0$ corresponds to a pair of independent harmonic oscillators with frequencies ω_1 and ω_2 corresponding to the normal modes perpendicular to and parallel to the magnetic field, respectively. Thus the first-order energy is

$$\epsilon_0 = \left(\nu_1 + \frac{1}{2}\right)\omega_1 + \left(\nu_2 + \frac{1}{2}\right)\omega_2 - \frac{1}{2\rho_m^2}, \quad (4)$$

where eigenstates are labeled by harmonic quantum numbers ν_1 and ν_2. In the strong-field limit, these correspond to the usual Landau (N) and "one-dimensional Coulomb" (ν) quantum numbers, respectively. In the weak-field limit, $D = 3$ states may be labeled by n, k, and m [13], where n is the principal quantum number and k labels the energy level ordering for fixed n and m. The correspondences with ν_1 and ν_2 are $n - k - |m| - 1$ and k, respectively. For instance, $|\nu_1\nu_2\rangle = |00\rangle$ corresponds at $D = 3$ to the $|nk|m|\rangle = |100\rangle = 1s_0$ state when $\kappa = 2$, the $|201\rangle = 2p_{\pm1}$ states when $\kappa = 4$, the $|302\rangle = 3d_{\pm2}$ states when $\kappa = 6$, and so on, i.e., the circular states.

Expanding the wave function and energy in Eq. (3) as

$$\epsilon = V_{\rm eff}(\rho_m,0) + \delta \sum_{j=0}^{\infty} \epsilon_{2j}\,\delta^j, \quad (5)$$

$$\Phi(x_1,x_2) = \sum_{j=0}^{\infty} \Phi_j(x_1,x_2)\,\delta^{j/2} \quad (6)$$

leads to an infinite set of coupled differential equations for $\Phi_j(x_1,x_2)$ and ϵ_{2j}, which may be efficiently computed [6] using a recently developed linear algebraic method [5].

Some general features may be deduced from the analytic expressions given above for perturbation theory through first order. In the $D \to \infty$ limit, all eigenstates collapse to the minimum of $V_{\rm eff}$. This minimum gives the correct energy for the lowest (nodeless) state in each azimuthal manifold in the zero-field limit and tends to the continuum threshold $E = (|m| + 1)\,B/2$ in the strong-field limit [4,6]. The complete degeneracy is lifted by the first-order term, in which perpendicular and parallel motions enter as normal modes of vibration. The adiabatic approximation has been used extensively in early studies of the strongly magnetized hydrogen problem. With the present method a similar separation enters naturally as a starting point for the subsequent $1/\kappa$ expansion, along with the correct Landau energy $(2N + |m| + 1)\,B/2$ contribution to the total energy through first order as $B \to \infty$. A first-order energy level diagram for even-parity states [$\pi_z = (-1)^{\nu_2} = +1$] with $\nu_1 + \nu_2 = n - |m| - 1 \le 10$ is shown in Fig. 1. This diagram, which represents the level structure in the large $|m|$ limit, bears some resemblance to exact energy level spectra for lower $|m|$ states [14] except that the avoided crossings are replaced by level crossings. These intersections occur at the locations where the ratio $\omega_1 : \omega_2$ is rational, such as $\tilde{B} \simeq 32.1$, where $\omega_1 = 2\omega_2$. Because of the harmonic approximation of the potential in the z direction, states which have several quanta in this normal mode are less well described by a first-order treatment. For instance, only three states (instead of all $|0\nu_2\rangle$ states) remain below the continuum threshold at the strongest field strength shown here.

The qualitatively correct results from the first two terms can be improved upon by including higher order terms. For states with small $|m|$, $1/\kappa$ at $D = 3$ is quite large and for all but the smallest B these asymptotic series require

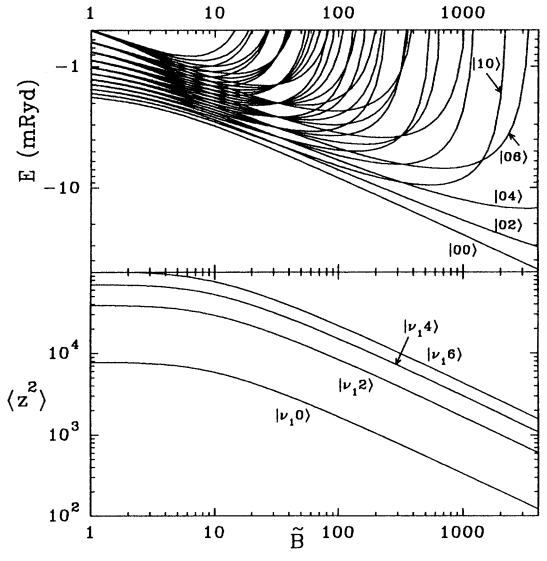

FIG. 1. Energy relative to ionization threshold and expectation value $\langle z^2\rangle$ through first order as a function of $\tilde{B}$, for the $m = -24$ even-parity manifold.

sophisticated summation methods such as Padé or Padé-Borel. However, for the CRS considered here, $1/\kappa$ is sufficiently small that simple partial sums yield highly accurate results except in the immediate vicinity of avoided crossings. In Table I we present the first few partial sums for the energy (including the normal Zeeman term) of the $m = -24$ CRS with $B = 3 \times 10^{-4}$ ($\approx$70.5 T). This is the smallest $|m|$ and strongest B for a CRS reported in the large scale calculations by Wunner *et al.* [11], and is chosen because it is the one for which DPT does poorest. Nonetheless, by fourth order the variational result is reproduced, and at tenth order we obtain convergence to machine accuracy (double precision).

In Fig. 2 we plot the energy for the lowest four even-parity states in the $m = -24$ manifold as a function of $\tilde{B}$. This may be compared with Fig. 1 of Ref. [11]. Series were computed through 20th order (1 min on a SPARCstation 1+) and convergent Padé approximants were plotted. Padé summation is used rather than partial sums since it does a much better job of summing series for the more highly excited states. The Padé sums of the energy may cross diabatically instead of displaying avoided crossings. When this happens the Padé approximants behave erratically in the heart of the avoided crossing. Such behavior has been noted before [15]. Here we simply join the curves on either side of the intersection, where the Padé approximants do not converge, with dotted lines so as to preserve the "no crossing" rule.

If the quantum numbers $|\nu_1 \nu_2\rangle$ are used to label the character, rather than the large dimension behavior, then this labeling passes through avoided crossings diabatically (see the discussion of expectation values below) with the result that they follow the pattern set by first-order perturbation theory. Indeed the actual avoided crossing involving $|10\rangle$ and $|02\rangle$ occurs not far from $\tilde{B} \simeq 32$, where the first-order calculation predicts a crossing.

One advantage of the linear algebraic method [5] is that the wave function terms Φ_j of Eq. (6) are directly computed in a basis of independent harmonic oscillators. From these expansions, we may compute the coefficients of series in powers of δ for expectation values [5]. As shown in Table I, the rate of convergence of the partial sums is comparable to that for the energy series. Because the $\kappa \to \infty$ circular orbit lies in the $z = 0$ plane, the series for $\langle z^2 \rangle$ begins at first order. In Figs. 1 and 2 we also plot $\langle z^2 \rangle$ as a function of $\tilde{B}$, exhibiting the quality of the first-order approximation which is especially good for the $|00\rangle$ CRS. As for the energies, we plot convergent Padé approximants through 20th order. If, in the vicinity of an avoided crossing in the energy plot, the Padé sums of $\langle z^2 \rangle$ fail to converge, we connect with dotted lines the same set of states that were joined in the energy plot.

The curves for $\langle z^2 \rangle$ cross at magnetic field strengths where the energy levels have avoided crossings, as one would expect from an exchange of character forced by the no crossing rule. Plots of $\langle \rho^2 \rangle$ (not shown) also exhibit the same behavior. The avoided crossings (character exchanges) are isolated and usually sharp at

TABLE I. Partial sums for the $m = -24$ circular state energy and expectation value $\langle z^2 \rangle$ at a field strength of $B = 3 \times 10^{-4} \simeq 70.5$ T ($\tilde{B} = 37.5$). The series for $\langle z^2 \rangle$ begins with the first-order term, and both series are unchanged (to the number of digits shown) beyond 12th order.

Order	$E(10^{-3}$ Ry)	$\langle z^2 \rangle$
0	−5.076 181 876 237 13	
1	−5.014 796 998 599 69	3086.414 795 836 26
2	−5.015 918 889 892 29	3207.951 676 065 63
3	−5.015 899 510 826 58	3209.095 452 458 65
4	−5.015 899 705 161 41	3209.077 579 145 55
5	−5.015 899 713 911 55	3209.078 138 849 00
6	−5.015 899 712 980 01	3209.078 120 371 57
7	−5.015 899 713 037 12	3209.078 120 433 78
8	−5.015 899 713 034 87	3209.078 120 527 51
9	−5.015 899 713 034 82	3209.078 120 512 36
10	−5.015899 713 034 84	3209.078 120 514 11
11	−5.015 899 713 034 84	3209.078 120 513 95
12+	−5.015 899 713 034 84	3209.078 120 513 96
Ref. [11]	−5.015 899 7	

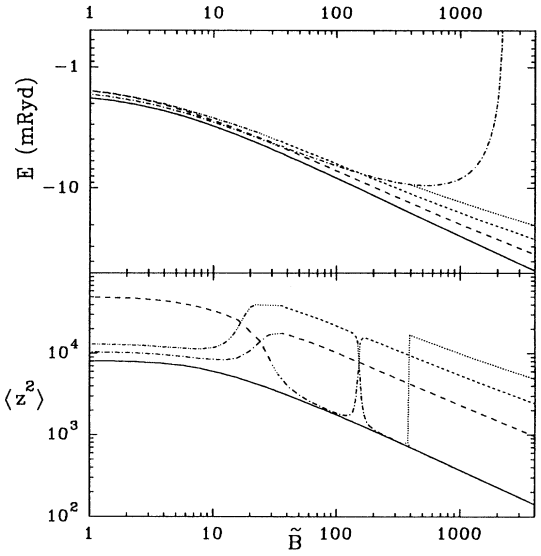

FIG. 2. Energy relative to ionization threshold and expectation value $\langle z^2 \rangle$ for the four lowest circular and nearly circular levels in the $m = -24$ even-parity manifold. Also shown for stronger field strengths is the lowest excited Landau level, $|\nu_1 \nu_2\rangle = |10\rangle$. The plots are drawn according to the quantum numbers $|\nu_1 \nu_2\rangle$, which denote the character of the state: $|00\rangle$, solid; $|02\rangle$, long dashed; $|04\rangle$, medium dashed; $|06\rangle$, short dashed; $|10\rangle$, dot-dashed; and $|20\rangle$, dot-dot-dashed. Limiting the plots to the four lowest states simplifies the figure, although some states carrying the $|20\rangle$, $|04\rangle$, and $|06\rangle$ quantum numbers over portions of the plots are excluded.

these magnetic field strengths and energies. This is to be expected since the perturbation parameter δ is small, with the result that wave functions and energies lie close to the large κ harmonic approximation except at avoided crossings, at least for states with small values of ν_1 and ν_2. Thus the quantum numbers $|\nu_1 \nu_2\rangle$ characterizing a state run diabatically through an avoided crossing. For example, in the avoided crossing near $\tilde{B} \simeq 25$ the lowest excited state changes from $|10\rangle$ with no excitation parallel to the field to $|02\rangle$ with two quanta of excitation parallel to the field, and consequently a larger $\langle z^2 \rangle$. Somewhat sharper is the crossing near $\tilde{B} \simeq 154$, where $|10\rangle$ and $|04\rangle$ exchange identities. By an infinite series of such exchanges, the $|10\rangle$ Landau state is promoted step by step until it eventually passes into the continuum. However, except at field strengths very close to the crossings, $\langle z^2 \rangle$ for the $|10\rangle$ state is always very close to that for the ground state ($|00\rangle$). This is expected from wave functions that are approximately separable in the ρ and z coordinates since neither state has any quanta in the ν_2 mode parallel to the field. Similar behavior is seen in plots of $\langle \rho^2 \rangle$ (not shown). Although it predicts the correct qualitative behavior for weak, intermediate, and strong B fields, the harmonic approximation becomes increasingly poor as the excitation rises. Despite this, the Padé sums of the perturbation series are still strongly convergent at $D = 3$ unless we are close to an avoided crossing. Thus we see that $\langle z^2 \rangle$ and $\langle \rho^2 \rangle$, as probes of the character of the wave function, demonstrate that the quantum numbers ν_1 and ν_2 may be used to label the states from weak to strong fields, correlate with quantum numbers of the weak- and strong-field limits and reflect the structure of the wave function.

We have shown that DPT provides a natural means to study circular and nearly circular Rydberg states. For these states the rapid convergence of the Padé sums and, for the circular states, partial sums yield highly accurate results with low order calculations. The quantum numbers ν_1 and ν_2 that emerge naturally from the large dimension analysis are seen to be approximate quantum numbers for these states from weak to strong fields in physical three-dimensional space and correlate with quantum numbers of the weak- and strong-field limits. Because both energy and wave function series can be computed, this method is well suited to the study of other properties, such as oscillator strengths. Also, the ease with which higher order perturbation coefficients may be computed permits the study of the large-order behavior of these series, which in turn should allow the calculation of complex energies from real series and the accurate calculation of the magnitude of avoided crossings [14,16].

T. C. G. acknowledges the award of a DOE Computational Science Graduate Fellowship. This work was supported by NSF Grant No. PHY-9123199.

[1] *Dimensional Scaling in Chemical Physics,* edited by D. R. Herschbach, J. Avery, and O. Goscinski (Kluwer, Dordrecht, 1992).
[2] D. Z. Goodson, M. López-Cabrera, D. R. Herschbach, and J. D. Morgan, III, J. Chem. Phys. **97**, 8481 (1992).
[3] V. M. Vaĭnberg, V. S. Popov, and A. V. Sergeev, Sov. Phys. JETP **71**, 470 (1990); also Ref. [1], Sect. 5.3 and 6.2.
[4] C. M. Bender, L. D. Mlodinow, and N. Papanicolaou, Phys. Rev. A **25**, 1305 (1982).
[5] M. Dunn, T. C. Germann, D. Z. Goodson, C. A. Traynor, J. D. Morgan, III, D. K. Watson, and D. R. Herschbach, J. Chem. Phys. **101**, 5987 (1994).
[6] T. C. Germann, D. R. Herschbach, and B. M. Boghosian, Comput. Phys. (to be published).
[7] R. G. Hulet and D. Kleppner, Phys. Rev. Lett. **51**, 1430 (1983).
[8] L. Chen, M. Cheret, F. Roussel, and G. Spiess, J. Phys. B **26**, L437 (1993), and references cited therein.
[9] R. G. Hulet, E. S. Hilfer, and D. Kleppner, Phys. Rev. Lett. **55**, 2137 (1985).
[10] Z. Dačić Gaeta and C. R. Stroud, Jr., Phys. Rev. A **42**, 6308 (1990); M. Mallalieu and C. R. Stroud, Jr., Phys. Rev. A **49**, 2329 (1994).
[11] G. Wunner, M. Kost, and H. Ruder, Phys. Rev. A **33**, 1444 (1986).
[12] W. Rösner, H. Herold, H. Ruder, and G. Wunner, Phys. Rev. A **28**, 2071 (1983).
[13] E. A. Solov'ev, JETP Lett. **34**, 265 (1981); D. R. Herrick, Phys. Rev. A **26**, 323 (1982); D. Delande and J. C. Gay, J. Phys. B **17**, L335 (1984); D. Wintgen and H. Friedrich, J. Phys. B **19**, 991 (1986).
[14] M. L. Zimmerman, M. M. Kash, and D. Kleppner, Phys. Rev. Lett. **45**, 1092 (1980).
[15] L. E. Fried and G. S. Ezra, J. Chem. Phys. **90**, 6378 (1989); D. Delande and J. C. Gay, J. Phys. B **19**, L173 (1986).
[16] D. Delande and J. C. Gay, Phys. Lett. **82A**, 393 (1981).